Petronio, C. and Weeks J.R.
Osaka J. Math.
37 (2000), 453–466

PARTIALLY FLAT IDEAL TRIANGULATIONS OF CUSPED HYPERBOLIC 3-MANIFOLDS

CARLO PETRONIO and JEFFREY R. WEEKS

(Received July 9, 1998)

1. Introduction

In his pioneering work [3], Thurston constructed a hyperbolic structure on the complement of the figure-eight knot by realizing it as the union of two regular ideal tetrahedra in $\mathbb{H}^3$ glued along faces. Since then, ideal triangulations have become an important instrument for constructing and studying finite-volume cusped hyperbolic 3-manifolds. However it is still not known whether such a manifold always admits geodesic ideal triangulations. Epstein and Penner [2] have shown that decompositions into convex ideal geodesic polyhedra always exist, but in general, if one subdivides the polyhedra into tetrahedra, some flat tetrahedra may be required to reconcile the subdivisions of adjacent polyhedra. Therefore if a manifold has a cusped finite-volume hyperbolic structure then it admits a *degenerate* geodesic ideal triangulation, in which some (but not all) of the tetrahedra are flattened out to quadrilaterals. A consequence of the main result of this paper is the converse to this statement. Actually, it is commonly conjectured, as the experimental evidence coming from [5] also suggests, that a *genuine* ideal triangulation always exists. Significant steps toward this conjecture were recently made by Wada, Yamashita and Yoshida, [6] and [7], but the full question appears to be still open.

Let M be the interior of a compact manifold whose boundary consists of tori and/or Klein bottles (this topological condition is known to be verified if M admits a complete finite-volume hyperbolic structure). Choose a topological ideal triangulation τ of M. Such triangulations always exist; one way to prove it is to note that they are dual to standard spines, which exist by [4]. Let τ consist of n tetrahedra. Then, using the combinatorial data which define τ, one can write down two systems of equations $\mathcal{C}$ and $\mathcal{M}$ in n complex variables (called respectively the *compatibility* and *completeness* equations) such that the following holds (see for instance [1]): *M admits a hyperbolic structure with respect to which τ can be isotoped to a geodesic ideal triangulation if and only if the system $(\mathcal{C}, \mathcal{M})$ admits a solution in π_+^n.* We recall that the open upper half-plane π_+ is the space of moduli of ideal tetrahedra in $\mathbb{H}^3$. Moreover, given $z \in \pi_+^n$, the system $\mathcal{C}(z)$ is satisfied if and only if the hyperbolic structure defined on the tetrahedra of τ by the moduli $z_1, \ldots, z_n$ is compatible with a (possibly incomplete) hyperbolic structure on M, and $\mathcal{M}(z)$ is satisfied if and only if such a structure is actually complete.

Let us define $\delta = \mathbb{R} \setminus \{0, 1\}$, and note that $\pi_+ \cup \delta$ is the space of moduli of ideal tetrahedra in $\mathbb{H}^3$, including those which flatten into 2-dimensional quadrilaterals with distinct vertices. The main result of this paper is the following:

Theorem 1.1. *If $z \in (\pi_+ \cup \delta)^n \setminus \delta^n$ and $(\mathcal{C}(z), \mathcal{M}(z))$ are satisfied then M admits a complete finite-volume hyperbolic structure obtained by gluing together in pairs the faces of the tetrahedra with moduli $z_1, \dots, z_n$ (some but not all of which may be flat).*

As announced above, from Theorem 1.1 and the result of Epstein and Penner we deduce:

Corollary 1.2. *A manifold M as above admits a complete finite-volume hyperbolic structure if and only if there exists a topological ideal triangulation τ of M such that the corresponding system of equations $(\mathcal{C}, \mathcal{M})$ admits a solution in $(\pi_+ \cup \delta)^n \setminus \delta^n$, where n is the number of tetrahedra in τ.*

What was most surprising to us, rather than the fact that Theorem 1.1 is true, is that its proof does not (and cannot) follow the lines of the proof in the case of solutions in π_+^n. Namely we show:

Proposition 1.3. *Let M and τ be as above and let $z \in (\pi_+ \cup \delta)^n \setminus \delta^n$ be a solution of $\mathcal{C}$. Then gluing together in pairs the faces of tetrahedra with moduli $z_1, \dots, z_n$ does not in general lead to an (even incomplete) hyperbolic structure on M.*

The remarkable phenomenon which occurs in the setting of the previous proposition is that, even if the compatibility equations are verified, the identification space which one gets by gluing the tetrahedra is not homeomorphic to M. This corresponds to the fact that the deformation of the genuine tetrahedra into flat ones cannot be performed within M.

Section 2 proves preparatory 2-dimensional analogues of Theorem 1.1 and Proposition 1.3. The 3-dimensional versions are proved in Sections 3 and 4, respectively.

2. The 2-dimensional case

We start by recalling that the system of hyperbolicity equations $(\mathcal{C}, \mathcal{M})$ mentioned in the introduction admits an interpretation on the boundary of the manifold M. First, note that π_+ is also the space of moduli of Euclidean triangles up to similarity (actually, just as for tetrahedra, we should fix an orientation and a basepoint on the triangle, but we will always leave this in the background). A topological ideal triangulation of M induces a triangulation of ∂M, and the choice of moduli $z_1, \dots, z_n \in \pi_+$ identifies the triangles on ∂M with Euclidean triangles up to similarity. Now, $\mathcal{C}(z)$ holds if

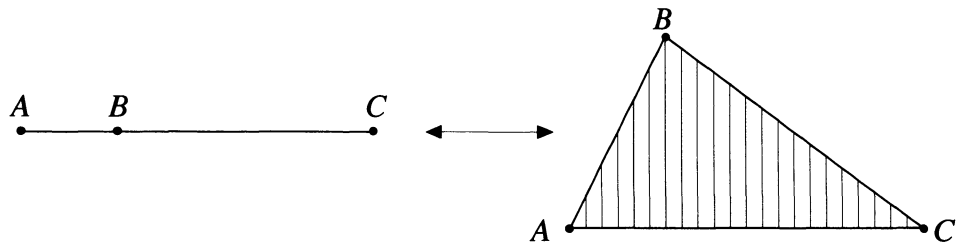

Fig. 1. Foliation of a triangle which corresponds to its degeneration

and only if this similarity structure on the triangles is compatible with a global similarity structure on ∂M, and $(\mathcal{C}(z), \mathcal{M}(z))$ holds if and only if this similarity structure is actually induced by a Euclidean structure.

Our first step is to prove that if one accepts solutions $z \in (\pi_+ \cup \delta)^n \setminus \delta^n$ then the system $\mathcal{C}(z)$ does not imply that ∂M has a natural similarity structure induced by z. Actually we will confine ourselves to a purely 2-dimensional situation (but the 3-dimensional counterexample of Section 4 will include the 2-dimensional counterexample on its boundary).

For later purpose it is convenient to formalize the situation. Let us consider a compact surface Σ without boundary. We will be mostly interested in the case that Σ is a torus or Klein bottle, but we allow any closed surface. Let σ be a triangulation of Σ. We will always allow triangles to have self-adjacencies and multiple adjacencies. The triangulation σ provides a recipe for constructing Σ by gluing together in pairs the edges of finitely many abstract triangles. Note that as soon as one specifies which edges are glued to which and in what direction, the resulting space is always Σ, independently of the gluing functions themselves. Now assume that some of the triangles degenerate into segments, i.e. the interior is removed and two of the edges are identified with proper subintervals of the third edge. Then we can still glue together the "edges" of the triangles coherently with the pairing previously used, but two new phenomena can occur:

1. The topological space resulting from the gluings may not be homeomorphic to Σ. This is obvious for instance if all triangles are degenerate; less trivial examples will be given later.
2. The topology of the resulting space depends in general on the gluing functions used. Explicit examples of this will be provided.

We can describe the degeneration in a useful alternative way. We consider the initial non-degenerate triangulation σ of Σ, and we foliate each triangle of σ corresponding to an abstract flat triangle, as suggested by Fig. 1. Moreover we arrange the relative position of the triangles of σ in such a way that adjacencies correspond exactly to the gluings of the (possibly flat) abstract versions. The result is a foliation-like partition of a portion of Σ. (It may not be a true foliation, because several leaves could

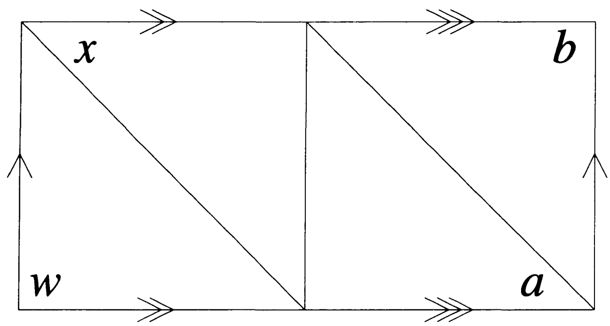

Fig. 2. A counterexample to compatibility in 2 dimensions

be incident to a vertex.) The identification space associated to the degeneration of the triangulation is obtained by collapsing each "leaf" to a point.

Now we turn to a geometric setting, starting from the Euclidean situation, which is relevant for the hyperbolic 3-dimensional case. So, we assume a correspondence to be given between the triangles of σ and the (possibly degenerate) Euclidean triangles with moduli $(z_1, \ldots, z_n) \in (\pi_+ \cup \delta)^n$ (recall that $\delta = \mathbb{R} \setminus \{0, 1\}$ corresponds to degenerate triangles). Now the ambiguity concerning the gluing functions between edges can be removed by choosing restrictions of Euclidean similarities.

Recall that the modulus of a Euclidean triangle with respect to one of its vertices is defined, and the compatibility equations $\mathcal{C}(z)$, for $z \in \pi_+^n$, express the fact that the product of moduli around each vertex of the triangulation is 1, and the sum of the corresponding arguments is 2π. Our first example shows that a solution z of $\mathcal{C}$ in $(\pi_+ \cup \delta)^n \setminus \delta^n$ may define an identification space not homeomorphic to Σ.

Proposition 2.1. *Choose any $a, b \in (0, 1)$ and $w \in \pi_+$ and set $x = (a(1-b)(1-w))^{-1}$. Then $x \in \pi_+$. Moreover, if in the triangulation of the torus described by* Fig. 2 *we choose a, b, x, w as moduli for the triangles as shown in the figure, then the corresponding identification space is non-Hausdorff.*

Proof of 2.1. We only need to construct the foliation, which we do in Fig. 3. The left side of the figure is drawn so as to indicate how the triangles flatten as the foliation collapses. The figure is drawn for the specific case that $a = b = 1/2, w = (1 + i\sqrt{23})/6, x = (5 + i\sqrt{23})/2$, but is topologically correct for all allowed values. (The seemingly crazy value for w is chosen for its later significance in the 3-dimensional case in Section 4.) Note too that the figure uses curvilinear edges to portray the flat triangles without making them disappear entirely. The right side of Fig. 3 is topologically the same as the left side, but has been drawn so that the gluing of each pair of edges is a Euclidean translation. This makes it easy to trace each leaf of the foliation as it wraps around the torus, as shown in Fig. 4.

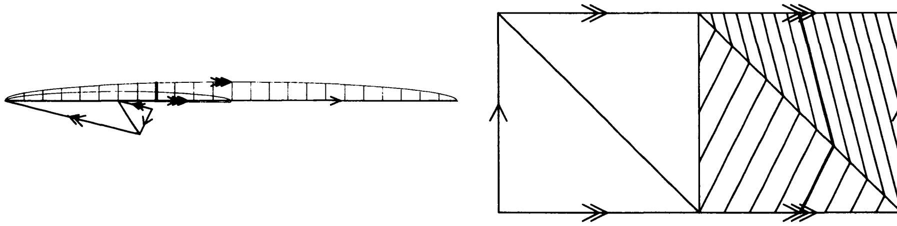

Fig. 3. Geometrical and topological pictures of the foliation on the fundamental domain

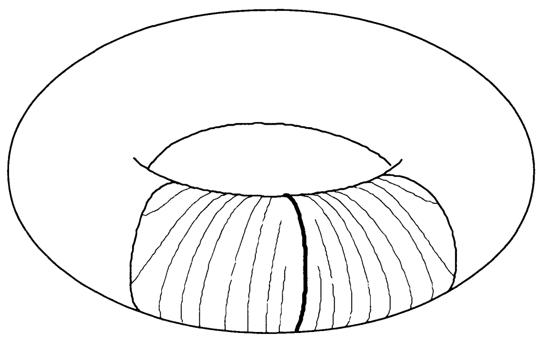

Fig. 4. The foliation on the torus

It easily follows from the figure that the identification space is a disjoint union of a cylinder and a point, where every neighbourhood of the point contains both the boundary circles of the cylinder, whence the conclusion. □

Before proceeding let us notice that using the same degenerate triangles as in the previous proposition, but different gluing functions, we can get a variety of non-homeomorphic identification spaces (e.g. with several "special" points).

We will show in the rest of this section that if $\mathcal{M}(z)$ also holds then the phenomena of the above example cannot happen. Recall first that if $z \in \pi_+^n$ satisfies $\mathcal{C}(z)$ then the dilation component $h_z : H_1(\Sigma) \to \mathbb{C}_*$ of the holonomy of the corresponding similarity structure is well-defined, and $\mathcal{M}(z)$ is the system $h_z(\mu) = h_z(\lambda) = 1$, where (μ, λ) is a pair of generators of $H_1(\Sigma)$ (here Σ is necessarily the torus or the Klein bottle). We first note that a weaker condition than $\mathcal{M}(z)$ has a geometric interpretation which will naturally lead to a generalization.

Lemma 2.2. *If $z \in (\pi_+ \cup \delta)^n$ satisfies $\mathcal{C}(z)$ and $|h_z(\mu)| = |h_z(\lambda)| = 1$ then the size of the Euclidean triangles corresponding to z can be consistently chosen so that all edge gluings are restrictions of isometries (not of mere similarities).*

The proof is immediate and left to the reader. Now we can generalize the situation as follows: let $\mathbb{X}^2$ be one of the model geometries $\mathbb{H}^2$, $\mathbb{E}^2$ or $\mathbb{S}^2$. As above we consider a surface Σ with a triangulation σ, and we take a correspondence between the triangles of σ and (possibly degenerate) geodesic triangles in $\mathbb{X}^2$. We assume that:

1. Edges which are glued in σ correspond to segments of the same length.
2. The total angle around each vertex of σ is 2π.

Concerning the last condition, note that a degenerate triangle has angles $0, 0, \pi$. As above we can form an identification space by gluing together the degenerate geodesic triangles along isometries.

Theorem 2.3. *Under the above assumptions, if not all the triangles are degenerate then the identification space is homeomorphic to Σ and the triangulation defines on Σ a natural $\mathbb{X}^2$-structure.*

Proof of 2.3. Let us colour blue the triangles of σ which correspond to degenerate triangles, and red the other ones. Let us draw a heavy black line along the edges where blue meets red. The heavy black lines divide Σ into a finite number of monochromatic components. Moreover the blue components are naturally foliated: to see this, note that when a vertex lies inside a blue component then incident to it are exactly two angles π and some angles 0, which implies that the leaf through the vertex arrives from one of the angles π and leaves from the other.

Now we concentrate on one of the blue components B and prove that all the leaves of its foliation are segments which connect a point of the boundary with another point of the boundary.

Let p be any point on the boundary of B. We are going to construct not just a path along the leaf beginning at p, but a nice wide boulevard centered along that leaf. Choose the width w of the boulevard to be less than the length of the shortest edge in the triangulation. Hire a road crew, and give them the following instructions for constructing the boulevard.

Initial instruction. If the point p lies at a vertex, or if the distance from p to one of the endpoints of the edge containing p is less than $w/2$, then the road crew should construct an initial portion of the boulevard as shown in either Fig. 5–left or Fig. 5–right, according to whether the total angle inside B at the vertex is 0 or π, respectively. In the former case the boulevard is complete and the road crew is dismissed; in the latter case the crew continues on. Note that the width of the boulevard is not well-defined on Σ (because the interior of the triangles do not have a geometry), but it is on the intersection with the 1-skeleton: the sum of the lengths of the two segments at the head of the boulevard is w.

Continuing instruction. Each morning the road crew is to advance the boulevard across a new triangle. If they arrive at a single edge on the far side of that triangle (Fig. 6–left), they get the afternoon off (with pay). If, however, they encounter a vertex

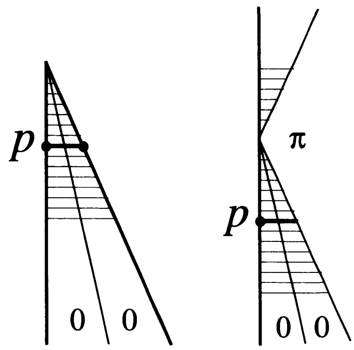

Fig. 5. First step in the construction of the boulevard

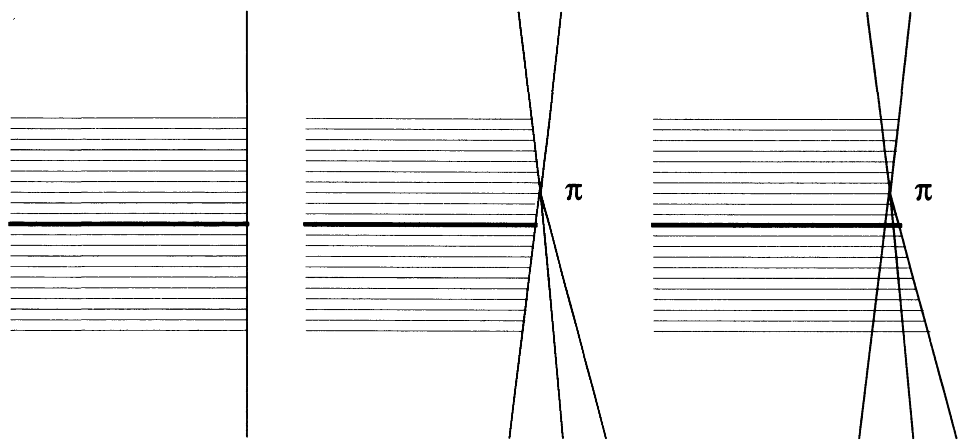

Fig. 6. Further steps in the construction of the boulevard

on the far side of the triangle (Fig. 6–centre), then in the afternoon they must extend the boulevard until they arrive at the other triangle with angle π incident to that vertex (Fig. 6–right). They never encounter more complicated situations, because the width of the boulevard is less than the shortest edge length.

What will happen when the road crew follows the above instructions? A priori there are three possibilities:

1. They could reach the red/blue boundary at a point p'.
2. They could encounter their own path.
3. They could work forever without encountering their own path.

We will prove that (2) and (3) are impossible, thereby arriving at the desired conclusion that the boulevard must reach some point p' on the red/blue boundary.

The crew cannot encounter their own path arriving at one of the edges of the

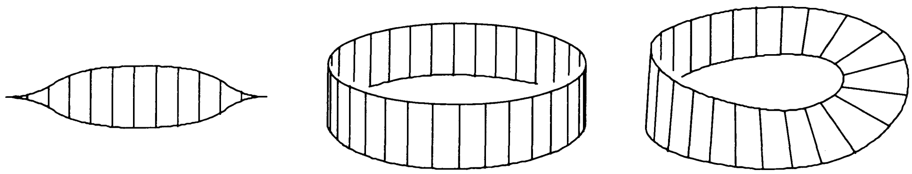

Fig. 7. Shape of the blue components

boulevard, because the boulevard is a union of parallel leaves. Moreover, the head of the boulevard under construction is always as portrayed in Figures 5 or 6, in particular it does not meet itself. This implies that the crew cannot meet their own path head on, proving that (2) is impossible.

The crew cannot work forever, because each morning the boulevard newly covers portions of edges of total length w, and the sum of the lengths of all edges in the triangulation is finite.

Therefore it follows that in a finite number of days the boulevard will terminate at a point p' on the red/blue boundary.

Now we can describe B in a more accurate way. If we start from a finite leaf and move one of its ends along ∂B at unit speed, then the other end also moves at unit speed. Therefore after a finite time one of the following happens:

1. The leaf disappears into a vertex of B at which B has internal angle 0, as in Fig. 5–left; in this case we move the leaf in the opposite direction and deduce that B is a bigon, as in Fig. 7–left.
2. The leaf comes back to itself; in this case, depending on orientation, B is a cylinder or Möbius strip as shown in Fig. 7–centre or right.

It is quite obvious that if the closure of a blue component appears in Σ as shown in Fig. 7, then we can squeeze the component along the leaves, leaving the topology unchanged. Moreover the geometric $\mathbb{X}^2$-structure previously defined near the boundary extends across the squeezed component. However in Fig. 7 we are showing the closure of the component B as an abstract surface: in Σ there could be self-adjacencies, and adjacencies of different components. On the other hand, recalling that the sum of angles at each vertex is 2π and that all the boundary angles of the red components are non-zero, one sees that the only possible adjacencies are as described in Fig. 8. Both types do no harm to the squeezing process, and the proof is complete. $\square$

Corollary 2.4. *If Σ is a triangulated torus or Klein bottle and $z \in (\pi_+ \cup \delta)^n \setminus \delta^n$ is a solution of the system $(\mathcal{C}, \mathcal{M})$ associated to the triangulation, then z defines a Euclidean structure on Σ up to change of scale.*

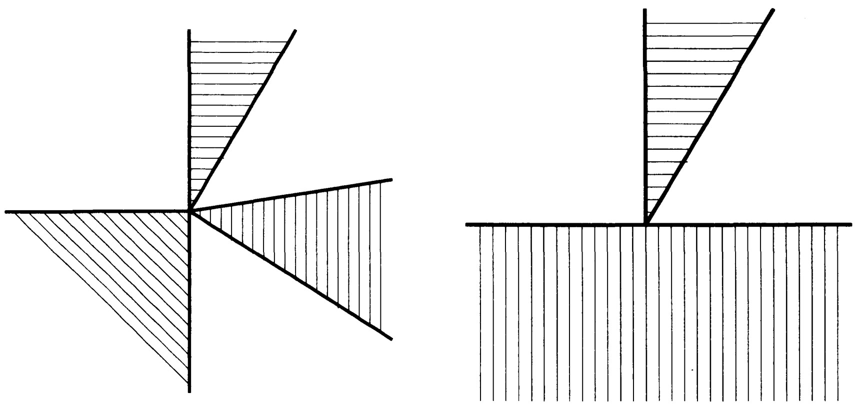

Fig. 8. Adjacencies of blue components

3. Hyperbolic 3-dimensional case: proof of the main result

This section is devoted to the proof of Theorem 1.1. The technique follows quite closely the 2-dimensional case treated in the previous section. We outline the various steps.

Step 1. *Initial setting and notation.* To start with, we view our manifold M as the interior of a compact manifold $\overline{M}$ with boundary, where $\overline{M}$ is (topologically) decomposed into truncated tetrahedra. As above we colour the tetrahedra blue and red and consider the 1-dimensional foliation of the blue components which translates the degeneration of the tetrahedra into quadrilaterals.

Note that the boundary $\partial\overline{M}$ inherits a triangulation to which Corollary 2.4 applies, and the picture we see on $\partial\overline{M}$ is exactly the same as in the proof of Theorem 2.3.

Step 2. *Geometry of the decomposition.* Before proceeding we need to be more precise about the geometry of the decomposition into truncated tetrahedra which we are considering. Recall that a geodesic ideal tetrahedron in $\mathbb{H}^3$ is truncated by removing (open) horoballs centred at its vertices. As we have already noticed in the previous section, if equations $(\mathcal{C}(z), \mathcal{M}(z))$ are satisfied then a consistent choice can be made of the size of the Euclidean triangles which get glued to give the boundary (we already know that the identification space is the boundary because of Corollary 2.4). Moreover, the Euclidean triangles are just intersections of tetrahedra with truncating horospheres, and the size of the triangle determines the height of the horosphere. Therefore the height of the various truncating horoballs can be chosen consistently with respect to the gluings. (Note that we still do not know that gluing the truncated tetrahedra gives $\overline{M}$: this is essentially what we have to prove.)

From what we have just said it follows that in the (partially foliated) decomposition of $\overline{M}$ all the hexagons (faces of the truncated tetrahedra) have a well-defined geometry. Namely, they are isometric to right-angled hexagons in $\mathbb{H}^2$ with edges which are alternatively geodesic and horocyclic arcs.

Step 3. *Finiteness of leaves, existence of tubes.* Let us concentrate on one of the blue components B. We first show that all the leaves which start at the boundary of B are finite and end on the boundary of B. This can be verified using basically the same argument as in the 2-dimensional case. Let $w > 0$ be small enough that every closed disc of radius w in $\mathbb{H}^2$ meets at most two different edges of the hexagonal faces in the decomposition of $\overline{M}$.

We can construct around a leaf γ which starts from the boundary of B a tube of radius w in which all the leaves are parallel to γ. Here the meaning of the radius of the tube, and the proof of its existence, are exactly as in the 2-dimensional case. The main point is that, by the choice of w, a cross-section parallel to γ always appears as in Fig. 6, in which vertices are intersections of the cross-section with a geodesic edge of the hexagons. Moreover, again by the choice of w, the local 3-dimensional picture of the tube is determined by the cross-section which contains γ, because nearby cross-sections are the same. Note that the cross-section orthogonal to γ of the tube is a hyperbolic disc of radius w, or such a disc minus a horodisc in case the tube intersects $\partial\overline{M}$.

The conclusion that γ is indeed finite is now proved by remarking that the total area of hexagonal faces is finite, and, as we proceed along γ, the tube covers at each step a definite portion of this area. To determine this portion a priori one has to use both w and the exact geometry of the hexagons. We will not do this explicitly.

We have shown that all the leaves which start at the boundary of B are finite and end on the boundary of B. We must now show that no other types of leaves occur, i.e. there are no circular or infinite leaves. To prove this, one may show that B is covered by the leaves which go from boundary to boundary. This is verified by checking that the union of leaves with ends on the boundary is both open and closed in B. Both properties are easily established using the tube of radius w described above.

Step 4. *Collapsibility of blue components.* We now note that each blue component B can be collapsed within $\overline{M}$ along its foliation. Note that, in contrast to the 2-dimensional case, infinitely many different shapes for B (with foliation as required) are possible. One could describe all of them quite easily, but we will not need to.

Step 5. *Conclusion.* In the previous step we have tacitly assumed that B is embedded in $\overline{M}$ without self-adjacencies. To conclude the proof, as in the previous section, one needs to note that the mutual and self-adjacencies of blue components are harmless when one actually collapses along the foliation, because locally they are just given by the 2-dimensional adjacencies of Fig. 8 multiplied by $\mathbb{R}$.

4. Hyperbolic 3-dimensional case: a counterexample to compatibility

This section extends the 2-dimensional counterexample from Section 2 to a hyperbolic 3-dimensional counterexample. More precisely, we provide a triangulated manifold and a choice of moduli satisfying the compatibility equations but not the com-

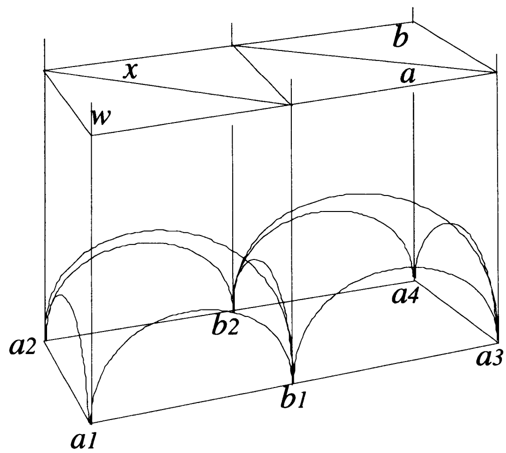

Fig. 9. The vertical faces of the four ideal tetrahedra are glued in the obvious straight-across way, while the four bottom faces are glued as $a_2a_1b_1 \leftrightarrow b_2a_3b_1$ and $b_1b_2a_2 \leftrightarrow a_3b_2a_4$.

pleteness equations, such that the corresponding foliation has infinite leaves. Collapsing the leaves of the foliation changes the topology of the manifold, which proves Proposition 1.3.

The triangulation is constructed in a straightforward way from the 2-dimensional triangulation shown in Figures 2 and 3. Namely, one lays the picture from Fig. 2 or 3 on the horizontal boundary plane of the upper half-space model of $\mathbb{H}^3$, and places an ideal tetrahedron over each triangle in the obvious way, that is, with three ideal vertices lying at the vertices of the triangle, and the fourth at infinity. The vertical faces of the tetrahedra are glued according to the edge gluings of the 2-dimensional case. Their bottom faces are glued according to Fig. 9. The resulting manifold will be denoted by M; it is a 2-cusp oriented manifold, and appears as the manifold $m129$ in the census of the computer program SnapPea [5].

It is straight-forward to verify that the moduli $a = b = 1/2$, $w = (1 + i\sqrt{23})/6$, $x = (5 + i\sqrt{23})/2$ satisfy the compatibility equations for both the "vertical" edges (corresponding to the vertices in the 2-dimensional case) and the "horizontal" edges (which have no analogue in the 2-dimensional case). Fig. 9 does not represent this particular solution, even though it gives a topologically accurate description of the manifold. To get an accurate idea of the geometry of this particular solution, the reader should imagine the four ideal tetrahedra sitting over the four triangles in the left side of Fig. 3, with a result as shown in Fig. 10.

As we saw in Sections 2 and 3, the effect of flattening some of the tetrahedra may be understood by analyzing the corresponding foliation. Fig. 10 shows the foliation in the two "flat" tetrahedra in M. Geometrically, of course, those two tetrahedra should

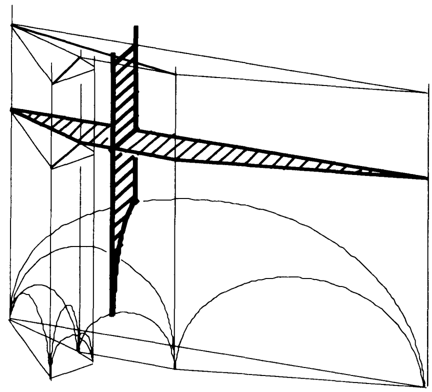

Fig. 10. The foliation of the two (almost) flat tetrahedra consists of horizontal segments orthogonal to the plane in which the tetrahedra (almost) lie. For clarity the segments are shown only in a typical horizontal cross-section and a very special vertical cross-section, namely the one which contains infinite leaves.

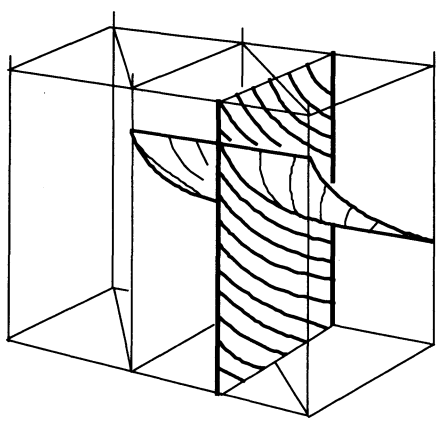

Fig. 11. A topological picture of the foliation

be drawn completely flat, but Fig. 10 gives them a small thickness, so as to provide a topologically accurate picture. Fig. 11 is topologically the same as Fig. 10, but has been drawn so that the gluing of each pair of vertical faces is a horizontal Euclidean translation. This makes it easy to trace each leaf of the foliation as it wraps around the manifold, and in particular to recognize that the vertical cross-section consists of infinite leaves.

We will denote by X the space obtained by collapsing each leaf of the foliation to a point, and endow it with the quotient topology. A careful analysis of the foliation, which we omit, leads to the following result:

Theorem 4.1. *Let $\overline{M}$ be the compact manifold with boundary whose interior is M. Then X is homeomorphic to the union of M and a simple loop $C \subset \overline{M} \setminus M$, with the topology induced by $\overline{M}$.*

Recalling that M has two cusps, one deduces from Theorem 4.1 that X differs from M only near one of the cusps, namely the one to which the infinite leaves are approaching.

The reader may wonder whether the pathology described in Theorem 4.1 is due to the use of the quotient topology, and whether a different topology might avoid it. In particular one might wonder whether the hyperbolic structure on the tetrahedra induces a hyperbolic metric on the quotient. Unfortunately, the resulting "metric" defines a non-Hausdorff space, because distinct points of the loop C of Theorem 4.1 turn out to be zero distance apart. We omit the proof.

Having shown that indeed there exist solutions of the compatibility equations which lead to degenerate identification spaces, we state without proof the following result, according to which no such a degeneration can take place near a complete solution.

Proposition 4.2. *Let $z^{(0)} \in (\pi_+ \cup \delta)^n \setminus \delta^n$ be a solution of $\mathcal{C}$ and $\mathcal{M}$. Then there exists a neighbourhood U of $z^{(0)}$ in $(\pi_+ \cup \delta)^n \setminus \delta^n$ such that if $z \in U$ is a solution of $\mathcal{C}$ then the identification space corresponding to z is the original manifold M, on which z naturally defines an (incomplete, in general) hyperbolic structure.*

The motivation for considering solutions near a complete one is that in the case of triangulations with genuine positive-volume tetrahedra, by considering this type of solution, one can prove Thurston's hyperbolic Dehn surgery theorem. However, it could a priori happen (and probably does in some cases) that if we start with a partially flat solution $z^{(0)}$ of $\mathcal{C}$ and $\mathcal{M}$ then all solutions of $\mathcal{C}$ close enough to $z^{(0)}$, other than $z^{(0)}$ itself, necessarily involve some negative-volume tetrahedra. In other words a neighbourhood of $z^{(0)}$ in $(\pi_+ \cup \delta)^n \setminus \delta^n$ could contain no solution of $\mathcal{C}$ except $z^{(0)}$. This is why we have decided to omit the proof of Proposition 4.2. If one could extend this result to include the case of negative volumes, i.e. by taking U to be a neighbourhood of $z^{(0)}$ in $(\mathbb{C} \setminus \{0, 1\})^n$ rather than in $(\pi_+ \cup \delta)^n \setminus \delta^n$ only, then one could probably prove the hyperbolic surgery theorem along the same lines as for the case of genuine tetrahedra.

References

[1] R. Benedetti and C. Petronio: Lectures on Hyperbolic Geometry, Springer-Verlag, Berlin-Heidelberg-New York, 1992.

[2] D.B.A. Epstein and R. Penner: *Euclidean decomposition of non-compact hyperbolic manifolds*, J. Differential Geom. **27** (1988), 67–80.

[3] W.P. Thurston: *The geometry and topology of* 3*-manifolds*, Mimeographed notes, Princeton University Mathematics Department, 1979.

[4] B.G. Casler: *An embedding theorem for connected* 3*-manifolds with boundary*, Proc. Amer. Math. Soc. **16** (1965), 559–566.

[5] J.R. Weeks: *SnapPea: a computer program for creating and studying hyperbolic 3-manifolds*, freely available from: www.northnet.org/weeks

[6] H. Yoshida: *Ideal tetrahedral decompositions of hyperbolic* 3*-manifolds*, Osaka J. Math. **33** (1996), 37–46.

[7] M. Wada, Y. Yamashita and H. Yoshida: *An inequality for polyhedra and ideal triangulations of cusped hyperbolic* 3*-manifolds*, Proc. Amer. Math. Soc. **124** (1996), 3905–3911.

C. Petronio
Dipartimento di Matematica
Università di Pisa
Via F. Buonarroti, 2
I-56127 PISA
Italy
e-mail: petronio@dm.unipi.it

J.R. Weeks
15 Farmer Street
Canton NY 13617
U.S.A.
e-mail: weeks@nortnet.org